doi:10.1038/nature10367

Overcoming lability of extremely long alkane carbon–carbon bonds through dispersion forces

Peter R. Schreiner[1], Lesya V. Chernish[2], Pavel A. Gunchenko[2], Evgeniya Yu. Tikhonchuk[2], Heike Hausmann[1], Michael Serafin[3], Sabine Schlecht[3], Jeremy E. P. Dahl[4], Robert M. K. Carlson[4] & Andrey A. Fokin[1,2]

Steric effects in chemistry are a consequence of the space required to accommodate the atoms and groups within a molecule, and are often thought to be dominated by repulsive forces arising from overlapping electron densities (Pauli repulsion). An appreciation of attractive interactions such as van der Waals forces (which include London dispersion forces) is necessary to understand chemical bonding and reactivity fully. This is evident from, for example, the strongly debated origin of the higher stability of branched alkanes relative to linear alkanes[1,2] and the possibility of constructing hydrocarbons with extraordinarily long C–C single bonds through steric crowding[3]. Although empirical bond distance/bond strength relationships have been established for C–C bonds[4] (longer C–C bonds have smaller bond dissociation energies), these have no present theoretical basis[5]. Nevertheless, these empirical considerations are fundamental to structural and energetic evaluations in chemistry[6,7], as summarized by Pauling[8] as early as 1960 and confirmed more recently[4]. Here we report the preparation of hydrocarbons with extremely long C–C bonds (up to 1.704 Å), the longest such bonds observed so far in alkanes. The prepared compounds are unexpectedly stable—noticeable decomposition occurs only above 200 °C. We prepared the alkanes by coupling nanometre-sized, diamond-like, highly rigid structures known as diamondoids[9]. The extraordinary stability of the coupling products is due to overall attractive dispersion interactions between the intramolecular H···H contact surfaces, as is evident from density functional theory computations with[10] and without inclusion of dispersion corrections.

"Matter will always display attraction" was J. D. van der Waals' favourite maxim[11], but this precept seems to have been partly forgotten. Literally stretching the limits of chemical bonding improves our understanding of the nature of stereoelectronic effects and the relative weights of covalent contributions relative to noncovalent contributions. General consensus exists regarding correlations between C–C bond lengths and their bond dissociation energies (BDEs) for a broad range of strained and unstrained compounds: shorter bonds are considered stronger, and vice versa. However, there are many exceptions to this relationship for bonds between elements other than carbon, emphasizing that there is no generalizable physical basis for this assumption[5]. Although practically all of these exceptions rely on the incorporation of highly electronegative atoms, we show here that alkanes with the longest C–C single bonds ever observed can still be quite stable. Such compounds can be realized by shifting the energy balance in favour of attractive dispersion interactions that outweigh to a large degree the repulsive dispersion contributions leading to C–C bond elongation. Our findings have consequences for understanding rotational barriers and thermodynamic preferences of branched alkanes over linear alkanes[1,2,12], and for the design of structures using attractive dispersion interactions. The examination of model systems to probe, rigorously understand and eventually control such 'hydrophobic interactions' (a term used in the life sciences) is key to advancing many aspects of molecular recognition.

The general recipe for elongating chemical bonds involves steric crowding[13]. This approach works well for, for example, structures **1**–**4** (Fig. 1), which have remarkably long C–C bonds, of up to 1.72 Å (C–C bond lengths of up to 1.78 Å have been reported for silicon-containing structures[14]), but reaches its limit of applicability with the highly crowded 'classic riddle'[15] hexaphenyl ethane (**5**, R = H), which has not yet been realized because its BDE apparently is too small (computed to be 17 kcal mol^{-1}; ref. 16) to allow its isolation. A bond length of 1.67 Å was determined experimentally[17] for persistent—yet sterically much more crowded—hexakis(3,5-di-*t*-butylphenyl)ethane (**5**, R = *t*-butyl (*t*-Bu)). Such low BDEs also result from benzylic resonance stabilization of the product triphenylmethyl radicals, whose formation is suppressed by holding the fragments in place through molecular bridges in the related compounds **3** and **4**[18].

The most sterically crowded alkanes prepared so far are **1**[19] and **2**[20], with C–C bonds of up to 1.65 Å. They are considered thermally labile, as expressed in the half-life of 1 h for **2** at 167 °C. Even more sterically crowed alkanes were deemed impossible because the BDEs for C–C bonds longer than 1.65 Å were empirically estimated to be around only 41 kcal mol^{-1} (refs 3, 4).

Our strategy to overcome the overall bond weakening through repulsive interactions is to design structures that additionally feature attractive dispersion interactions, by controlling the number and lengths of hydrogen–hydrogen van der Waals contacts surrounding each C–C bond under consideration. This idea is inconsistent with the general assumption that strained alkane C–C bonds are dominated by repulsive interactions[21], and we will use quantum chemical computations to show that the balance between repulsive and attractive van der

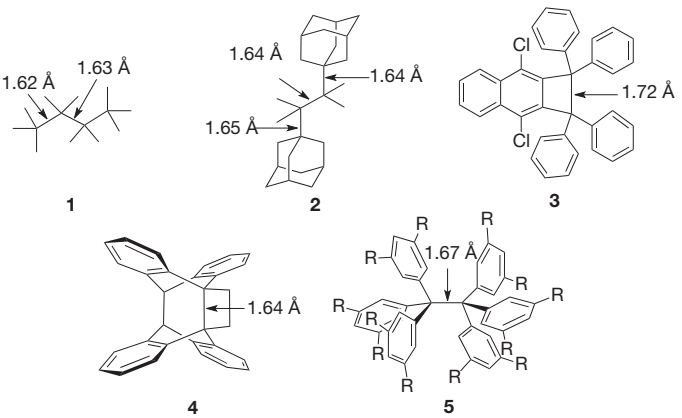

Figure 1 | Hydrocarbons with exceptionally long C–C bonds. Structures **1**–**4** have been reported experimentally; structure **5** (R = H) has not been observed but **5** (R = *t*-Bu) is experimentally known (bond length given). All of these structures are thermally labile and have half-lives of only a few hours upon moderate heating.

[1]Institut für Organische Chemie der Justus-Liebig-Universität, Heinrich-Buff-Ring 58, D-35392 Giessen, Germany. [2]Department of Organic Chemistry, Kiev Polytechnic Institute, 37 Pobeda Avenue, Kiev 03056, Ukraine. [3]Institut für Anorganische Chemie der Justus-Liebig-Universität, Heinrich-Buff-Ring 58, D-35392 Giessen, Germany. [4]Stanford University, Stanford Institute for Materials & Energy Science, 476 Lomita Mall, Stanford, California 94305, USA.

Waals interactions can be shifted significantly. We used this strategy to prepare alkanes with unprecedented thermal stability and C–C bond lengths. A second aspect of our strategy is that the radicals formed from C–C bond dissociation should be structurally very similar to the hydrocarbon moiety in the undissociated starting material, to avoid stabilization through interactions only present in the relaxed alkyl radical structures[22].

These considerations led us to the design and preparation of coupled diamondoid molecules because these have large, hydrogen-terminated contact areas (Fig. 2) and their corresponding tertiary radicals are structurally very similar to their hydrocarbon precursors, such that radical stabilization through geometrical relaxation is minimized. Diamondoids are nanometre-sized (0.4–1.2 nm), hydrogen-terminated, diamond-like alkanes that are available through synthesis (only for the smallest members of this family) or through isolation from petroleum[9]. These true nanodiamonds, of which adamantane is the smallest, consist of a series formed by adding adamantane subunits to a tetrahedral $C_{10}H_{16}$ core; the naming of the simplest nanodiamonds follows from the number of adamantane moieties[9] (diamantane, triamantane and so forth; Fig. 2).

The tertiary diamondoid bromides of hydrocarbons **6**–**8** (Fig. 2) readily undergo Wurtz coupling at 145 °C in xylene to give the heterodimers **7•7** (65%), **6•8** (25%) and **7•8** (21%) (where the point denotes the C–C bond), which were chemically fully characterized. All diamondoid adducts crystallize well and were subjected to X-ray analysis (Fig. 2), revealing extraordinarily long central C–C bonds (1.647–1.704 Å).

Notably, all three compounds have high melting points, and we assessed their thermal stability using differential scanning calorimetry (DSC) and thermogravimetric analyses (TGA). These analyses reveal that **7•7** is stable up to at least 300 °C and melts at about 360 °C. Similarly, **6•8** (melting point, 310 °C) slowly decomposes above 300 °C, whereas **7•8** begins decomposition at only 220 °C. The monitoring of the TGA experiments with a mass detector revealed that the volatile decomposition products are the parent hydrocarbons **6** and **7**. Such high melting points are typical for stable cage hydrocarbons such as the diamondoids (melting points: **6**, 270 °C; **7**, 244 °C; **8**, 225 °C), by marked contrast with the low melting points of conformationally flexible alkanes[23]. To quantify further the great stability of **7•8**, we determined the hydrogen transfer reaction energies in the presence of 9,10-dihydroanthracene[20] as a hydrogen donor in pressure-tight steel containers (for details, see Supplementary Figs 8 and 9 and Supplementary Table 1), finding a reaction enthalpy of −24.6 kcal mol^{-1} in the range of 190–210 °C. As the temperature for this hydrogentransfer reaction and the onset of decomposition of **7•8** are close, the activation free energy associated with this reaction ($\Delta G_{573}^{\ddagger} = 37.5 \pm 7.9$ kcal mol^{-1}) must be attributed to the interfragment C–C bond breaking in **7•8**. This is in line with the expectation that **7•8** is more stable than **2** ($\Delta G_{573}^{\ddagger} = 30.5$ kcal mol^{-1}), despite its considerably longer central C–C bond length.

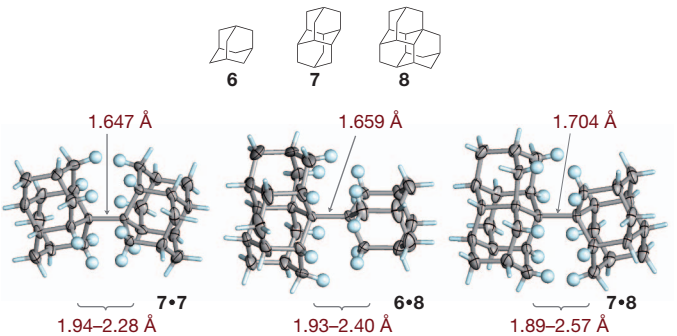

Figure 2 | Diamondoids and X-ray crystal structures of their coupling products with very long central C–C bonds. Adamantane (**6**), diamantane (**7**) and triamantane (**8**) as nanodiamond building blocks for their coupling products diamantane–diamantane (**7•7**), adamantane–triamantane (**6•8**) and diamantane–triamantane (**7•8**). The hydrogen-terminated surfaces are shown with the hydrogen atoms in light blue; the curly brackets indicate the distance ranges for the H···H contacts around the central C–C bonds.

The gas-phase stability of the heterodimers was also assessed by gas chromatography mass spectrometry measurements. For instance, **7•7** can readily be identified by its molecular ion mass peak, even at an inlet temperature of 280 °C and a retention time of 120 min.

From known C–C bond distance/bond energy correlations[4], these heterodimers are all expected to be thermally unstable. Hence, the lability of their central C–C bonds must be energetically overcompensated for by favourable bonding interactions. We therefore determined which interactions are responsible for the stabilities of **7•7**, **6•8** and **7•8**. The X-ray crystal structure analyses reveal that the lengths of the H···H contacts between the two hydrocarbon moieties are in the range of 1.9–2.6 Å, with the majority being around 2.2–2.3 Å. This corresponds well to the optimal H···H distances found for molecular crystals of many organic structures (2.2–2.4 Å; ref. 24); the H···H contacts in the adamantane X-ray crystal structure are 2.37–2.46 Å in length[25].

We also performed a computational analysis of **7•7**, in the same symmetry (C_2) as found in the X-ray structure, and of **5** using various density functional theory (DFT) approaches. As the standard implementation of DFT does not explicitly include dispersion interactions (for example in the popular B3LYP functional combination), this allows an analysis of the results by comparison with dispersion-corrected (DFT-D) levels of theory[10] (B3LYP-D). These results are compared with modern functionals that have been extensively reparameterized (for example M06; Table 1). To validate our computational approach, we computed the reaction enthalpy of the hydrogen transfer from 9,10-dihydroanthracene and found that our reference computations at B3LYP-D/6-31G(d,p) give −26.9 kcal mol^{-1} (at 200 °C), in excellent agreement with experiment (−24.6 kcal mol^{-1}), only on inclusion of dispersion interactions. Similar results were obtained with a modern functional (M06-2X; ref. 26) and another (B97D) that more properly account (to different degrees) for dispersion interactions (Supplementary Table 1). Neglect of dispersion, as in uncorrected B3LYP/6-31G(d,p), gives an error of nearly 30 kcal mol^{-1}.

The B3LYP-D and M06-2X approaches reproduce the central C–C bond distances quite well (an exact match cannot be expected because computed values inevitably differ slightly from the experimental data owing to approximations in the DFT formulations and the differences arising from gas-phase versus condensed-phase structures), lending credibility to the computations. For **7•7**, the inclusion of dispersion corrections increases the BDE significantly. A BDE of 71 kcal mol^{-1} for **7•7**, which is nearly 30 kcal mol^{-1} above the expected empirical value[4], is in agreement with the experimentally found high stability.

For **5** (R = H), inclusion of dispersion corrections reduces the BDE and increases the central C–C bond distance, whereas it significantly decreases that in **7•7**. This indicates the overall dominance of repulsive interactions between the neighbouring phenyl rings in **5** (R = H). Although the phenyl rings in **5** (R = H) have a favourable, distorted T-shape benzene dimer[27] orientation relative to each other, their attractive dispersion interactions are insufficient to allow the preparation and isolation of **5** (R = H) at ambient temperatures. Remarkably, the addition of all-*meta* *t*-Bu groups to give **5** (R = *t*-Bu) increases the BDE (relative to **5** (R = H)) and decreases the central C–C bond distance. Indeed, **5** (R = *t*-Bu) has been fully characterized by crystal structure analysis[17]. By contrast with **5** (R = H), the inclusion of dispersion corrections decreases the central C–C bond distance for **5** (R = *t*-Bu), as it does for **7•7**: This must be a consequence of attractive dispersion interactions resulting from addition of the *t*-Bu groups. Again, the H···H contact distances of the *t*-Bu groups in **5** (R = *t*-Bu) are around 2.1–2.5 Å, which is comparable to our heterodimer structures, demonstrating the similarities in the sources of their stabilization.

The notion of attractive rather than repulsive H···H contacts touches on many aspects of chemistry, biology and the materials sciences. For

Table 1 | The BDEs and C–C bond lengths of 7•7 and 5 computed at various levels of DFT

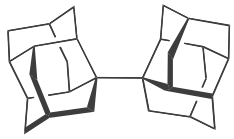

7•7

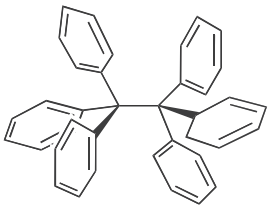

5 (R = H)

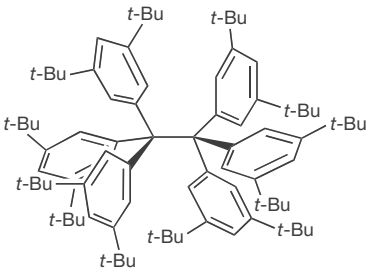

5 (R = *t*-Bu)

Method/quantity	BDE (kcal mol^{-1})	C–C (Å)	BDE (kcal mol^{-1})	C–C (Å)	BDE (kcal mol^{-1})	C–C (Å)
B3LYP/6-31G(d,p)	43.9	1.674	−20.9	1.730	−26.1	1.709
B3LYP-D/6-31G(d,p)	70.7	1.653	10.3	1.735	44.5	1.674
B97D/6-31G(d,p)	64.5	1.668	6.5	1.791	38.8	1.698
M06-2X/6-31G(d,p)	65.8	1.648	12.3	1.702	33.0	1.669
Experiment	—	1.647	—	—	—	1.670(3)

The experimental bond distance for **5** (R = *t*-Bu) is from ref. 17. Structures are drawn for best possible visibility. 'D' denotes a correction for dispersion energies; the M06-2X functional has been extensively reparameterized to include some amount of dispersion. The parenthetical uncertainty in the **5** (R = *t*-Bu) C–C bond length is the standard deviation in X-ray standard notation.

instance, protobranching, defined as net attractive 1,3-alkyl-alkyl stabilizing interactions, has been suggested (and criticized[12]) to be responsible for the higher thermodynamic stability of branched alkanes over unbranched alkanes[2]. It is likely that these overall stabilizing interactions receive large contributions from favourable H···H contacts. Another example is the 'corset effect', whereby apparent steric crowding around labile molecular moieties stabilizes the overall structure kinetically; a prime example is the preparation and isolation of tetra-*t*-butyltetrahedrane[28] (Supplementary Table 2; the less crowded parent hydrocarbon is yet unknown). This stabilization can alternatively be interpreted as arising from favourable van der Waals contacts of the *t*-Bu groups; this suggestion is supported by the value of −3.1 kcal mol^{-1} computed for the isodesmic equation 2 di-*t*-butyltetrahedrane → tetra-*t*-butyltetrahedrane + tetrahedrane at B3LYP-D/6-31G(d,p). Along these lines, it is notable that many recently discovered carbene-stabilized complexes also involve bulky pendant alkyl groups[29] that may contribute to the overall stabilization of these otherwise labile systems[30].

METHODS SUMMARY

The diamondoid heterodimers were prepared by refluxing the respective bromodiamondoid precursors in a small volume of dry *m*-xylene under argon atmosphere in the presence of sodium metal. After work-up and compound separation on silica gel, the final products were crystallized from *n*-hexane. Experimental details and compound characterizations are described in detail in Methods and Supplementary Information. DSC measurements were performed in platinum–corundum double-layer crucibles under argon. TGA analyses (coupled with a mass spectrometer) were conducted in corundum crucibles under argon atmosphere. All thermal analyses were temperature-calibrated. The X-ray crystallographic data for **7•7**, **6•8** and **7•8** were collected at 193 K using molybdenum Kα radiation and a graphite monochromator. The structures were solved by direct methods and refined by using full-matrix least-squares analyses; all non-hydrogen atoms were treated anisotropically. Importantly, all hydrogen atoms could be found in the difference Fourier syntheses and were refined isotropically.

The electronic structure computations were carried out with the Gaussian03 and Gaussian09 program suites. All structures were fully optimized and characterized as minima (by computing analytical second derivatives) of their respective potential energy hypersurfaces at the levels of DFT given in the text. All optimized geometries (*x*–*y*–*z* coordinates) and absolute electronic energies are given in Supplementary Table 3.

Full Methods and any associated references are available in the online version of the paper at www.nature.com/nature.

Received 11 January; accepted 15 July 2011.

1. Grimme, S. Seemingly simple stereoelectronic effects in alkane isomers and the implications for Kohn–Sham density functional theory. *Angew. Chem. Int. Ed.* **45,** 4460–4464 (2006).
2. Wodrich, M. D. *et al.* The concept of protobranching and its many paradigm shifting implications for energy evaluations. *Chem. Eur. J.* **13,** 7731–7744 (2007).
3. de Silva, K. M. N. & Goodman, J. M. What is the smallest saturated acyclic alkane that cannot be made? *J. Chem. Inf. Model.* **45,** 81–87 (2005).
4. Zavitsas, A. A. The relation between bond lengths and dissociation energies of carbon-carbon bonds. *J. Phys. Chem. A* **107,** 897–898 (2003).
5. Kaupp, M., Metz, B. & Stoll, H. Breakdown of bond length-bond strength correlation: a case study. *Angew. Chem. Int. Ed.* **39,** 4607–4609 (2000).
6. Gordy, W. A relation between bond force constants, bond orders, bond lengths, and the electronegativities of the bonded atoms. *J. Chem. Phys.* **14,** 305–320 (1946).
7. Huggins, M. L. Atomic radii. IV. Dependence of interatomic distance on bond energy. *J. Am. Chem. Soc.* **75,** 4126–4133 (1953).
8. Pauling, L. *The Nature of the Chemical Bond* (Cornell Univ. Press, 1960).
9. Schwertfeger, H., Fokin, A. A. & Schreiner, P. R. Diamonds are a chemist's best friend: diamondoid chemistry beyond adamantane. *Angew. Chem. Int. Ed.* **47,** 1022–1036 (2008).
10. Grimme, S. Accurate description of van der Waals complexes by density functional theory including empirical corrections. *J. Comput. Chem.* **25,** 1463–1473 (2004).
11. Tang, K.-T. & Toennies, J. P. Johannes Diderik van der Waals: a pioneer in the molecular sciences and Nobel prize winner in 1910. *Angew. Chem. Int. Ed.* **49,** 9574–9579 (2010).
12. Gronert, S. The folly of protobranching: turning repulsive interactions into attractive ones and rewriting the strain/stabilization energies of organic chemistry. *Chem. Eur. J.* **15,** 5372–5382 (2009).
13. Suzuki, T., Takeda, T., Kawai, H. & Fujiwara, K. Ultralong C–C bonds in hexaphenylethane derivatives. *Pure Appl. Chem.* **80,** 547–553 (2008).
14. Fritz, G., Wartanessian, S., Matern, E., Hönle, W. & von Schnering, H. G. Bildung siliciumorganischer Verbindungen. 85. Bildung, Reaktionen und Struktur des 1,1,3,3-tetramethyl-2,4-bis(trimethylsilyl)-1,3-disilabicyclo[1.1.0]butans. *Z. Allg. Anorg. Chem.* **475,** 87–108 (1981).
15. McBride, J. M. The hexaphenylethane riddle. *Tetrahedron* **30,** 2009–2022 (1974).
16. Vreven, T. & Morokuma, K. Prediction of the dissociation energy of hexaphenylethane using the ONIOM(MO: MO: MO) method. *J. Phys. Chem. A* **106,** 6167–6170 (2002).
17. Kahr, B., van Engen, D. & Mislow, K. Length of the ethane bond in hexaphenylethane and its derivatives. *J. Am. Chem. Soc.* **108,** 8305–8307 (1986).
18. Kammermeier, S., Jones, P. G. & Herges, R. [2+2] cycloaddition products of tetradehydrodianthracene: experimental and theoretical proof of extraordinary long C–C single bonds. *Angew. Chem. Int. Edn Engl.* **36,** 1757–1760 (1997).
19. Winiker, R., Beckhaus, H. D. & Rüchardt, C. Thermische Stabilität, Spannungsenthalpie und Struktur symmetrisch hexaalkylierter Ethane. *Chem. Ber.* **113,** 3456–3476 (1980).
20. Flamm-ter Meer, M. A., Beckhaus, H. D., Peters, K., von Schnering, H. G. & Rüchardt, C. Thermolabile hydrocarbons, XXVII. 2,3-di-1-adamantyl-2,3-dimethylbutane; long bonds and low thermal stability. *Chem. Ber.* **118,** 4665–4673 (1985).
21. Rüchardt, C. & Beckhaus, H. D. Towards an understanding of the carbon-carbon bond. *Angew. Chem. Int. Edn Engl.* **19,** 429–440 (1980).
22. Rüchardt, C. & Beckhaus, H.-D. Consequences of strain for the structure of aliphatic molecules. *Angew. Chem. Int. Edn Engl.* **24,** 529–538 (1985).
23. Boese, R., Weiss, H.-C. & Bläser, D. The melting point alternation in the short-chain *n*-alkanes: single-crystal X-ray analyses of propane at 30 K and of *n*-butane to *n*-nonane at 90 K. *Angew. Chem. Int. Ed.* **38,** 988–992 (1999).
24. Grimme, S. *et al.* When do interacting atoms form a chemical bond? Spectroscopic measurements and theoretical analyses of dideuteriophenanthrene. *Angew. Chem. Int. Ed.* **48,** 2592–2595 (2009).
25. Donohue, J. & Goodman, S. H. The crystal structure of adamantane: an example of a false minimum in least squares. *Acta Crystallogr.* **22,** 352–354 (1967).
26. Zhao, Y. & Truhlar, D. G. The M06 suite of density functionals for main group thermochemistry, thermochemical kinetics, noncovalent interactions, excited states, and transition elements: two new functionals and systematic testing of four M06-class functionals and 12 other functionals. *Theor. Chem. Acc.* **120,** 215–241 (2008).

27. Takatani, T. & Sherrill, C. D. Performance of spin-component-scaled Moller-Plesset theory (SCS-MP2) for potential energy curves of noncovalent interactions. *Phys. Chem. Chem. Phys.* **9,** 6106–6114 (2007).
28. Maier, G., Pfriem, S., Schäfer, U. & Matusch, R. Tetra-*tert*-butyltetrahedrane. *Angew. Chem. Int. Edn Engl.* **17,** 520–521 (1978).
29. Wang, Y. Z. & Robinson, G. H. Unique homonuclear multiple bonding in main group compounds. *Chem. Commun. (Camb.)* 5201–5213 (2009).
30. Dyker, C. A. & Bertrand, G. Soluble allotropes of main-group elements. *Science* **321,** 1050–1051 (2008).

Supplementary Information is linked to the online version of the paper at www.nature.com/nature.

Acknowledgements We thank S. Grimme for providing an implementation of his dispersion correction technique and for discussions. We are grateful for support from the Deutsche Forschungsgemeinschaft and the National Science Foundation of the USA, and in part from the Department of Energy, Office of Basic Energy Sciences, Division of Materials Science and Engineering, under contract DE-AC02-76SF00515; the Ministry of Science and Education of Ukraine; and the Ukrainian State Basic Research Fund.

Author Contributions P.R.S. and A.A.F. formulated the initial working hypothesis and provided, analysed and interpreted all experimental data. L.V.C, P.A.G. and E.Yu.T. carried out the coupling experiments. H.H. recorded and analysed all NMR data. M.S. solved all X-ray structures. S.S. provided and interpreted the DSC and TGA analyses. J.E.P.D. and R.M.K.C. isolated and purified the diamondoids. The manuscript was written by P.R.S. and A.A.F.

Author Information X-ray crystal structures have been deposited in the Cambridge Crystallographic Database under the deposition numbers CCDC 805315 (**7•7**), CCDC 806293 (**6•8**) and CCDC 806294 (**7•8**). Reprints and permissions information is available at www.nature.com/reprints. The authors declare no competing financial interests. Readers are welcome to comment on the online version of this article at www.nature.com/nature. Correspondence and requests for materials should be addressed to P.R.S. (prs@org.chemie.uni-giessen.de) or A.A.F. (aaf@xtf.ntu-kpi.kiev.ua).

METHODS

Diamondoid coupling procedure. For the Wurtz coupling, 1 mmol of the chosen bromodiamondoid precursors was dissolved in a small volume of dry *m*-xylene and refluxed (140–150 °C in the oil bath) in a two-neck flask fitted with an argon inlet and an anchor stirrer with an air-cooled condenser under a slow stream of argon. Small pieces of sodium (0.3 g, or 13 mmol, in total) were added to the stirred reaction mixture over 1.5 h. After adding all of the sodium, the mixture was refluxed for a total of 4 h and cooled to 50 °C; then the excess of sodium was quenched with methanol. After cooling to room temperature (23 ± 2 °C), the reaction mixture was filtered and washed with water, evaporated and separated on silica gel (*n*-hexane); the final products were crystallized from *n*-hexane. All compounds were characterized by nuclear magnetic resonance spectroscopy, high-resolution mass spectrometry, elemental analysis and X-ray crystal structure determination.

Computations. All geometries were fully optimized at the stated level of theory, described using the standard abbreviations: B3, Becke's three-parameter exchange functional[31]; LYP, Lee–Yang–Paar correlation functional[32]; D, dispersion correction according to refs 33, 34; M06-2X, Truhlar's high-nonlocality functional with double the amount of nonlocal exchange[26]; B97, Becke's 1997 exchange-correlation functional[35]. We used a standard 6-31G[36] basis set with polarization functions on carbon (d) and hydrogen (p). All structures were characterized as minima of their respective potential energy hypersurfaces by confirming that all computed harmonic vibrational frequencies are real. These frequencies were also used to derive zero-point vibrational energy corrections to the relative energies. We used the Gaussian03[37] (version D.02 for adding Grimme's dispersion correction to B3LYP) and the Gaussian09[38] programs (version B.01) for all computations.

Thermogravimetric and differential scanning calorimetric analyses. DSC measurements were performed in a Netzsch Pegasus 404 C calorimeter in platinum–corundum double-layer crucibles under an argon flow of 50 ml min^{-1} at a heating rate of 10 K min^{-1}. TGA analyses were conducted in a Netzsch Luxx STA 409 PC apparatus coupled to an Aëlos QMS 403 C mass spectrometer. The samples were heated in corundum crucibles in an argon atmosphere at a heating rate of 10 K min^{-1}. Both instruments were temperature-calibrated in the range from room temperature to 1,100 °C with standard element samples of indium, tin, bismuth, aluminium, silver and gold. The results for the compounds under consideration here are graphically summarized in Supplementary Figs 1–7. The reasons for the differences between the behaviour seen in Supplementary Fig. 2 and that seen in Supplementary Figs 1 and 3 can be found in the construction geometry of the apparatus used in our work. The TGA and mass spectrometry units are connected by a heated transfer line that is held at a temperature of 250 °C and is about 1 m in length. The volatile adamantane released from **6•8** can easily pass through this transfer line and is therefore detected as it forms. The much less volatile diamantane produced from **7•7** and **7•8** has to pass through the transfer line in stepwise sublimation processes and only reaches the mass spectrometer when the temperature at the TGA unit has reached a value much higher than 250 °C. The maximum concentration of diamantane is found at 550 °C in both Supplementary Fig. 1 and Supplementary Fig. 3. This is consistent with the formation of diamantane in both cases.

31. Becke, A. D. Density-functional thermochemistry. III. The role of exact exchange. *J. Chem. Phys.* **98,** 5648–5652 (1993).
32. Lee, C. T., Yang, W. T. & Parr, R. G. Development of the Colle-Salvetti correlation-energy formula into a functional of the electron-density. *Phys. Rev. B* **37,** 785–789 (1988).
33. Grimme, S. Semiempirical GGA-type density functional constructed with a long-range dispersion correction. *J. Comput. Chem.* **27,** 1787–1799 (2006).
34. Schwabe, T. & Grimme, S. Towards chemical accuracy for the thermodynamics of large molecules: new hybrid density functionals including non-local correlation effects. *Phys. Chem. Chem. Phys.* **8,** 4398–4401 (2006).
35. Becke, A. D. Density-functional thermochemistry. V. Systematic optimization of exchange-correlation functionals. *J. Chem. Phys.* **107,** 8554–8560 (1997).
36. Binkley, J. S., Pople, J. A. & Hehre, W. J. Split valence basis sets. *J. Am. Chem. Soc.* **102,** 939–947 (1980).
37. Frisch, M. J, *et al. Gaussian 03 v.D.02* (Gaussian, Inc., 2003).
38. Frisch, M. J, *et al. Gaussian09 v.B.01* (Gaussian, Inc., 2009).